Pure Appl. Geophys. 173 (2016), 1039–1050

DOI 10.1007/s00024-016-1256-5

Pure and Applied Geophysics

Chilean Earthquakes: Aquifer Responses at the Russian Platform

ALINA BESEDINA,[1] EVGENY VINOGRADOV,[1] ELLA GORBUNOVA,[1] and IGOR SVINTSOV[1]

Abstract—We studied hydrogeological responses to the passage of seismic waves from the Chilean earthquakes with Ms ≥7.6 at epicentral distances of about 126°. The variation in the levels of confined and unconfined aquifers was analyzed under platform conditions at the Mikhnevo Geophysical Observatory near Moscow, Russia. Synchronous recording of seismic and hydrogeological data enabled us to evaluate the amplitude–frequency response of aquifers. The study shows that medium response to dynamic impact depends on various physical parameters of the aquifers.

Key words: Confined and unconfined aquifers, distant Chilean earthquakes, seismic waves, hydrogeological response.

1. Introduction

On September 16, 2015 an earthquake occurred off the coast of Chile, with a magnitude Ms = 8.3 (Geophysical Survey of RAS http://www.ceme.gsras.ru/cgi-bin/ceme/info_quake.pl?mode=1&id=265), and caused a significant response of the aquifer within the Russian Platform, at a distance of over 14000 km from the epicenter. Recent papers confirmed co-seismic and post-seismic changes of well groundwater levels in different parts of the globe as a result of strong earthquakes. Based on seismic impact on the aquifer, pore fluid pressure is redistributed, which can lead to a change in reservoir structure (WANG2007) and permeability (ELKHOURY *et al.* 2006) and to the initiation of new seismic events (BRODSKY *et al.* 2003).

Hydrogeological response during the passage of a seismic wave may be divided into high-frequency oscillations and changes in the water level in the form of its rise or fall, which may be either transient or sustained (MONTGOMERY and MANGA 2003). A change in the properties of the underground reservoir rock and its consolidation may occur in the near and intermediate fields (MONTGOMERY and MANGA 2003; WANG 2007). In the far field of the earthquake, the most likely mechanism of water level fluctuations is reservoir rock deformation during propagation of a seismic wave (WANG and MANGA 2010).

With the participation of the authors, the hydrogeological response to the propagation of seismic waves from earthquakes with a magnitude of 7 or more was for the first time noted at teleseismic distances under the Russian Platform conditions (KOCHARYAN *et al.* 2011; BESEDINA *et al.* 2015). During a 7-year period of precision observations, amplitude variations of the groundwater level from earthquakes were comparable to hydrogeological responses to the stationary changes in atmospheric pressure and earth tides (BESEDINA *et al.* 2014), but for some cases it rises significantly during strong earthquakes. Previously, only the barometric and tidal components of groundwater level were taken into consideration for the Russian Platform (BAGMET *et al.* 1989; LYUBUSHIN *et al.* 1997). The values obtained were used to estimate reservoir rock properties.

The variation of groundwater level is studied predominantly in seismically active regions (BRODSKY *et al.* 2003; ELKHOURY *et al.* 2006; LIU *et al.* 2006; DOAN and CORNET 2007; SHI *et al.* 2015). Some authors (KANO and YANAGIDANI 2006) observed a frequency-independent response of the water level in a closed well with respect to ground velocity at frequencies below 0.2 Hz. The Sumatra–Andaman earthquake of 2004, however, was characterized by inverse frequency dependence (KITAGAWA *et al.* 2006). In an open well of the confined aquifer near

[1] Institute of Geosphere Dynamics, Russian Academy of Sciences, 38 Leninskiy Prosp., Bldg. 1, Moscow 119334, Russian Federation. E-mail: besedina.a@gmail.com

Grants Pass, Oregon, a constant amplification factor was recorded at teleseismic earthquakes for frequencies below 0.05 Hz. For regional events, there is a reverse frequency dependence of the amplification factor of the well (Brodsky *et al.* 2003).

Existing studies are often contradictory, thus our results add data of recorded variations in platform conditions and expand the global database of hydrogeological observations. In the study, we determine the reaction of water level in open wells under confined and unconfined conditions to remote earthquakes that occurred off the west coast of Chile.

2. *Observational Data and Research Methods*

We review the water level change as a response to remote earthquakes in two open wells that were drilled within the territory of the Mikhnevo Geophysical Observatory (54.96N. lat. 37.77E. long., central part of the Russian Platform, 80 km to the South from Moscow; international code—MHV). The Middle carboniferous Kashira deposit is penetrated in the interval of 46.0–56.6 m and the Lower carboniferous Aleksin deposit is penetrated in the interval of 92–115 m. The distance between wells is 30 m. Figure 1 shows the geological cross section. Aquifers are separated by Middle carboniferous Vereya horizon, a regional aquiclude. Moscow artesian basin that contains MHV territory is a complex multilayer system of aquifers and aquicluding aquitards. Unconfined Kashira aquifer (C_2kš) spreads overall besides the Valley of Oka River with branches where it is eroded (Fig. 2). Underground water flow has a radial orientation and relatively high velocity. Confined Aleksin aquifer (C_1al) has a north-east orientation and total immersion with slope up to 0.001. The main aquifers parameters are shown in Table 1; there and elsewhere, we note confined Aleksin aquifer C_1al as WLC and unconfined Kashira aquifer C_2kš as WLU and use the same abbreviations for appropriate wells and data.

Precision observation of groundwater level change in the well was conducted by LMP308i submersible precision digital level sensors with a 2 mm accuracy and sampling rate of 1 Hz. The confined aquifer response has been recorded since 2008 and

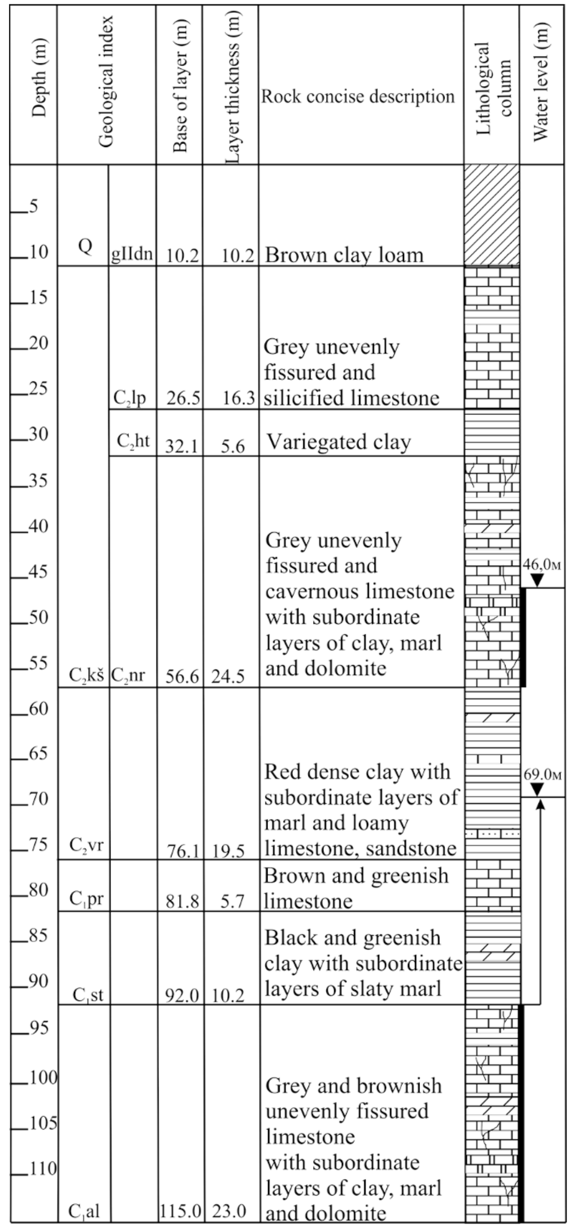

Figure 1
Geological cross section

that of the unconfined aquifer since 2013. Water-bearing rocks are represented by unevenly fissured limestone with subordinate layers of clay, marl and dolomites and are considered reservoirs of a fracture-pore type.

Seismic ground motions were recorded by an STS-2 three-component broadband seismometer (MHV), located in the mine at a depth of 22 m. The seismic

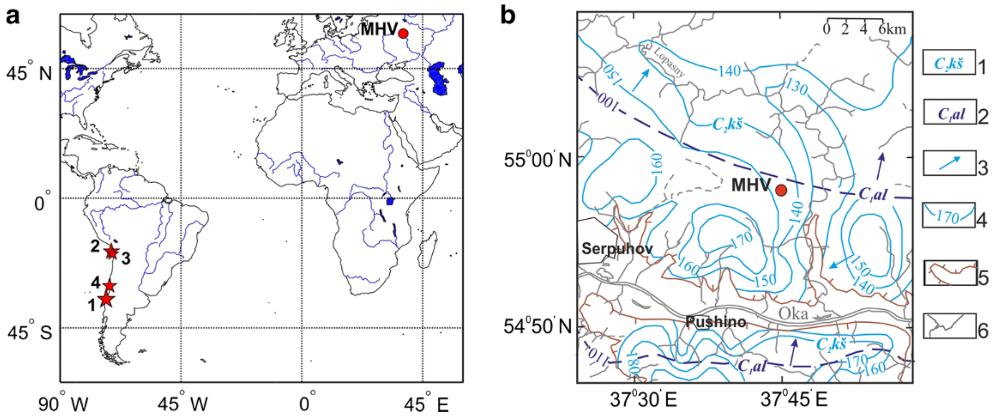

Figure 2

a Location of MHV with regard to the Chile earthquake epicenters: *1* February 27, 2010, Ms = 8.7; *2* April 1, 2014, Ms = 8.0; *3* April 3, 2014, Ms = 7.6; *4* September 16, 2015, Ms = 8.3. **b** Hydrogeological scheme of the surrounding area of MHV: *1*, *2* the prevalence area of Kashira and Aleksin aquifers, respectively; *3* the main direction of Kashira (*light blue*) and Aleksin (*deep blue*) aquifers; *4* the absolute grade (m) of hydroisohypse; *5* the boundaries of regional aquiclude; *6* the river system

Table 1

Well parameters

Variable	WLC (confined Aleksin aquifer)	WLU (unconfined Kashira aquifer)
Well bore radius (m)	0.059	0.056
Well casing radius (m)	0.0635	0.0585
Well depth (m)	115	60.5
Penetrated aquifer thickness (water influx interval) (m)	23	12
Water level in well from the surface (m) (September 16, 2015)	69	46
Pressure head (m)	23	–
Transmissivity (m^2/day)	4.0	15.0
Hydraulic conductivity (m/day)	0.17	1.5
Specific storage (m^{-1})[a]	36.9×10^{-7}	–

[a] Theoretically estimated in (Kopylova *et al.* 2009)

station records seismic events in the range of 0.0083–50 Hz, with a 100 Hz analog-to-digital converter sampling rate. For comparison with hydrogeological data, the sampling rate of the seismic data was preliminarily reduced by a factor of 100. The amplitude and phase responses of STS-2, built on the values of zeroes [0; 0] and poles [$-0.037 + 0.037i$; -0.037 to $0.037i$], are shown in Fig. 3 (black line). Comparison of hydrogeological and seismic data of remote earthquakes with periods of more than 10 s indicates the need for correction of the broadband seismometer phase characteristics, since for the waves with a period of 50 s, the phase shift is 6 s, and for the 100—22 s (Fig. 3, black line). Constructing an inverse digital filter (Scherbaum 1996) to restore the frequency components attenuated to the noise level leads to a considerable increase of noise dispersion in which the useful signal may become completely lost (Besedina 2014). Instead of it, we restored the STS-2 frequency characteristics to 1200 s (Fig. 3, red line) by multiplying the transfer function of the sensor by a correction filter that is described by zeros [$-0.037 + 0.037i$; -0.037 to $0.037i$] and poles [$-0.0037 + 0.0037i$; -0.0037 to $0.0037i$].

To remove any artifacts that may be generated by restoring the frequency characteristic of STS-2 to 1200 s, low-cut filter with cutoff frequency of 0.0025 Hz was performed. The described procedure allowed the STS-2 phase response to be taken into consideration and the phase shift to be reduced to 2 s for a wave with a period of 100 s, and to less than 1 s for a wave with a period of 50 s. For adequate comparison, the data of the water level in wells were also cleared of the long-period trend higher than 400 s.

According to the catalog of the Geophysical Service of the Russian Academy of Sciences (GS RAS http://www.gsras.ru), nine Chilean earthquakes with a magnitude $7.1 \leq Ms \leq 8.7$ were recorded in 2010–2015 (Table 2). The water level in the well monitors the hydrostatic head pressure of the well, which changes due to the deformation of the massif during the passage of a seismic wave. In the quasi-elastic medium, changes in water level are determined by dynamic stresses, or by peak ground velocity (PGV). The characteristic parameter of the well's response to the passage of seismic waves is the amplification factor, defined as the ratio of the water level variation amplitude to the ground velocity. The well amplification factor can be calculated by dividing the observed spectra of the groundwater level variations in the well by the ground velocity. The spectrum of ground velocity and water level fluctuations in a 10800 s recording was calculated using the Welch method (sliding Hanning window with duration of 1350 s, with 50 % overlap) (Welch 1967). To plot the frequency–time diagrams, we used the program Spectra Analyser by A.A.Lyubushin (http://www.ifz.ru/applied/analiz-dannykh-monitoringa/programmnoe-obespechenie/, manual in Russian). The initial data were decimated by a factor of 3 because of program limit for window length and then the Morlet wavelet $\psi(t) = \frac{1}{\pi^{1/4}} \cdot exp\left(-t^2/2 - i\pi t\right)$ was used to build diagrams.

3. Measurement Results

Variations in the level of the confined and unconfined aquifers were observed only during the passage of seismic waves from four distant

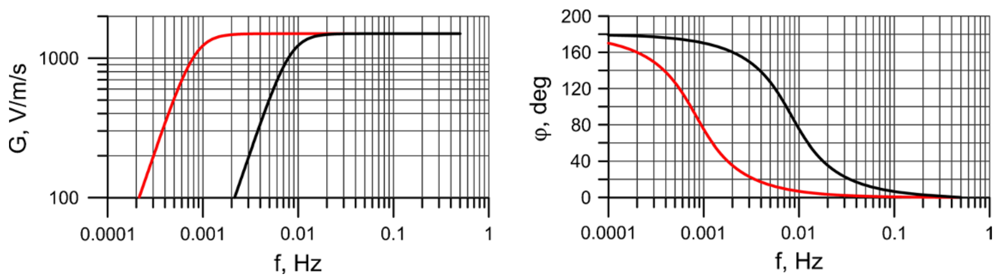

Figure 3
Amplitude–frequency (*left*) and phase–frequency (*right*) characteristics: STS-2 broadband seismometer (period of oscillation 120 s), represented by the *black line*; STS-2 seismometer with characteristics expanded into lower frequencies (oscillation period 1200 s), represented by the *red line*

Table 2

Earthquakes confined to the coast of Chile, according to the catalog of GS RAS, from 2010 until the present

No.	Date	Time at the epicenter [GMT]	Lat	Lon	Epicentral distance (km)	Depth (km)	Ms
1	2010-02-27	06:34:13.0	−36.04	−72.88	14477	33	8.7
2	2010-03-11	14:39:48.0	−34.42	−71.88	14285	33	7.1
3	2010-03-11	14:55:29.1	−34.44	−71.89	14287	33	7.1
4	2011-01-02	20:20:16.3	−38.37	−73.44	14694	15	7.2
5	2011-02-11	20:05:29.8	−36.61	−72.99	14529	20	7.1
6	2012-03-25	22:37:06.7	−35.17	−71.94	14349	33	7.2
7	2014-04-01	23:46:46.9	−19.60	−70.95	12969	20	8.0
8	2014-04-03	02:43:13.5	−20.50	−70.46	13017	20	7.6
9	2015-09-16	22:54:30	−31.6	−71.61	14038	25	8.3

Table 3

Parameters of ground velocity and level response

No.	Date	GVZ (mm/s)	T_{Seism} (LR) (s)	WLU (mm)	T_{WLU} (LR) (s)	WLC (mm)
1	2010-02-27	1.74	25	–	–	14.9
8	2014-04-01	0.42	20	15.1	20	–
9	2014-04-03	0.32	21	13.3	21	–
10	2015-09-16	0.58	21	23.1	20	3

earthquakes with Ms $\geq$7.6 magnitude (Nos. 1, 7, 8 and 9 of Table 2), occurring near the west coast of Chile from 2010 onward. Table 3 shows the maximum amplitude (double PGV—from the highest to the lowest) of the ground velocity and hydrogeological response of the aquifers as well as the main visible period of maximum oscillation.

Figure 4 shows the earthquake seismograms and level fluctuations in the observation wells. We analyzed Z-, E- and N-components of seismic data for February 27, 2010 and September 16, 2015 earthquakes and Z- and E-components for April 1, 2014 and April 3, 2014 earthquakes because of technical problems with the N-channel.

The hydrogeological response of the lower confined aquifer was observed during two earthquakes with the largest magnitudes Ms = 8.7 on February 27, 2010 and Ms = 8.3 on September 16, 2015. In the first case, the level changes relate to the passage of the transverse and surface waves (Fig. 4a), and in the second to the arrival of surface waves (Fig. 4d). The longitudinal wave amplitude is too small for the existing capacity of registration.

Hydrogeological response to three earthquakes was observed in the unconfined aquifer (Table 2, Nos. 7, 8, 9) (Fig. 4). Level variations relate both to transverse and surface waves. The maximum amplitude variation was observed on September 16, 2015.

Figures 5 and 6 show the 2-D frequency–time diagrams of the seismic Z-component and water level variations for earthquakes that occurred on February 27, 2010 and September 16, 2015. Palettes are not identical for more clear view inside every single diagram and due to negligibility of absolute amplitude values. The red line marks the PKiKP wave arrival and this moment is considered as a null point. Wavelet analysis shows wave arrivals noted above and clearly demonstrates wave dispersion both in seismic records and water level oscillations.

The signal and background spectra for the September 16, 2015 earthquake (epicentral distance is 14000 km) are compared by evaluating 3 h before PKiKP arrival and 3 h after PKiKP arrival. The main periods of the seismic waves were identified in the range of less than 0.2 Hz (Fig. 7a), whereas level variations of the confined and unconfined aquifer have periods below 0.014 and 0.08 Hz accordingly (Fig. 7b, c).

A comparative analysis of an earthquake and a natural microseismic background spectra makes it possible to remove the influence of the local topography of the station. Figure 8 shows the spectral ratio of the earthquake spectra (3 h after PKiKP arrival) to the natural microseismic background (3 h before PKiKP arrival) for four Chilean earthquakes (Table 2, Nos. 1, 7, 8, 9). Frequencies of the significant peaks that match in seismic and water level records are marked with color signs and red lines. An amplification factor, i.e., the ratio of the level changes to peak ground velocity, was estimated for every single noted frequency peak (Fig. 9). This value characterizes aquifer hydrogeological response to remote earthquakes. For the three earthquakes discussed (Table 2, Nos. 7, 8, 9), the average value of the WLU amplification factor is constant in the period range of 15–40 s and equals to 39 mm/mm/s at teleseismic distances with a root-mean-square deviation of 3 mm/mm/s. The WLC amplification factor calculated for two earthquakes (Table 2, Nos. 1, 9) is about 6 mm/mm/s with a root-mean-square deviation of 1 mm/mm/s (orange point at 0.048 Hz is excluded from averaging).

4. Discussion

We recorded the hydrogeological response of the level of confined and unconfined aquifers in a geodynamically stable platform during the passage of seismic waves from a large earthquakes that occurred on the other side of the world—off the coast of Chile.

Under confined conditions, the dynamic response of the water level to seismic action is well known (Cooper *et al.* 1965) and is often used to estimate

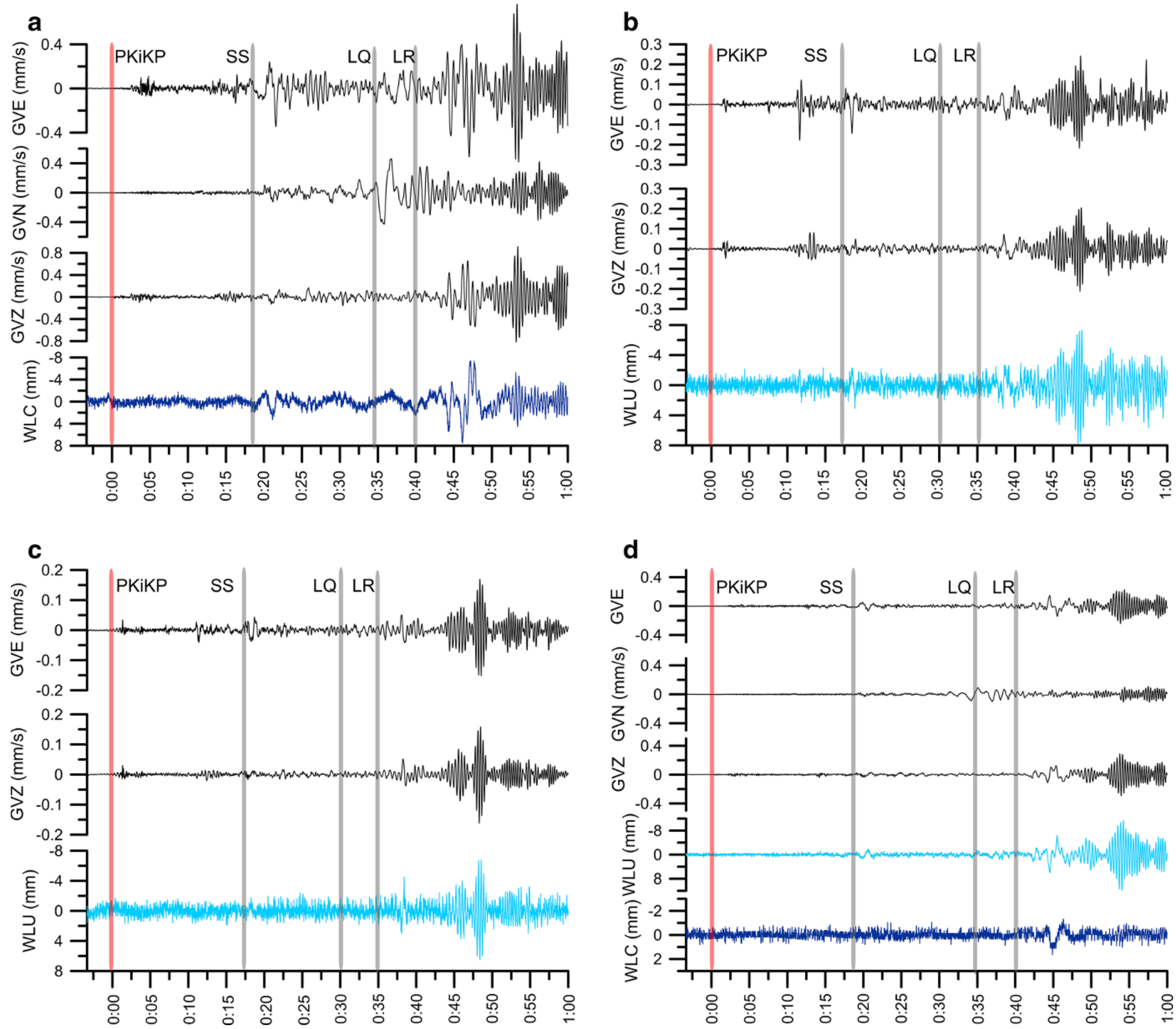

Figure 4
Seismograms of earthquakes and water level variations: **a** February 27, 2010, Ms = 8.7; **b** April 1, 2014, Ms = 8.0; **c** April 3, 2014, Ms = 7.6; **d** September 16, 2015, Ms = 8.3. *GVE* ground velocity east, *GVN* ground velocity north, *GVZ* vertical ground velocity, *WLC* water level of confined aquifer (*deep blue*), *WLU* water level of unconfined aquifer (*light blue*). Body wave arrivals are marked as PKiKP (longitudinal wave) and SS (transverse wave). Surface wave arrivals are marked as LQ (Love wave) and LR (Rayleigh wave). Wave arrivals are determined by IASP 91 Earth model. We consider PKiKP wave arrival as a null point

reservoir rock properties, for example, by Doan *et al.* (2006). Significantly less publications observe unconfined aquifer response to seismic waves. The porosity of the reservoir rock under unconfined conditions may be evaluated based on the water level, the volume deformation and aquifer thickness (Bredehoeft 1967; Brown *et al.* 2005). Simultaneous monitoring of the water level of confined and unconfined aquifers allows the development of a holistic view of the filtration parameters of the studied massif. It is known that the amplitude variations in the groundwater level caused by the earthquake are determined by the relationship between the magnitude and epicentral distance (Montgomery and Manga 2003).

We recorded the response of the unconfined aquifer upon the arrival of the transverse wave and a group of surface waves. Earthquake to natural

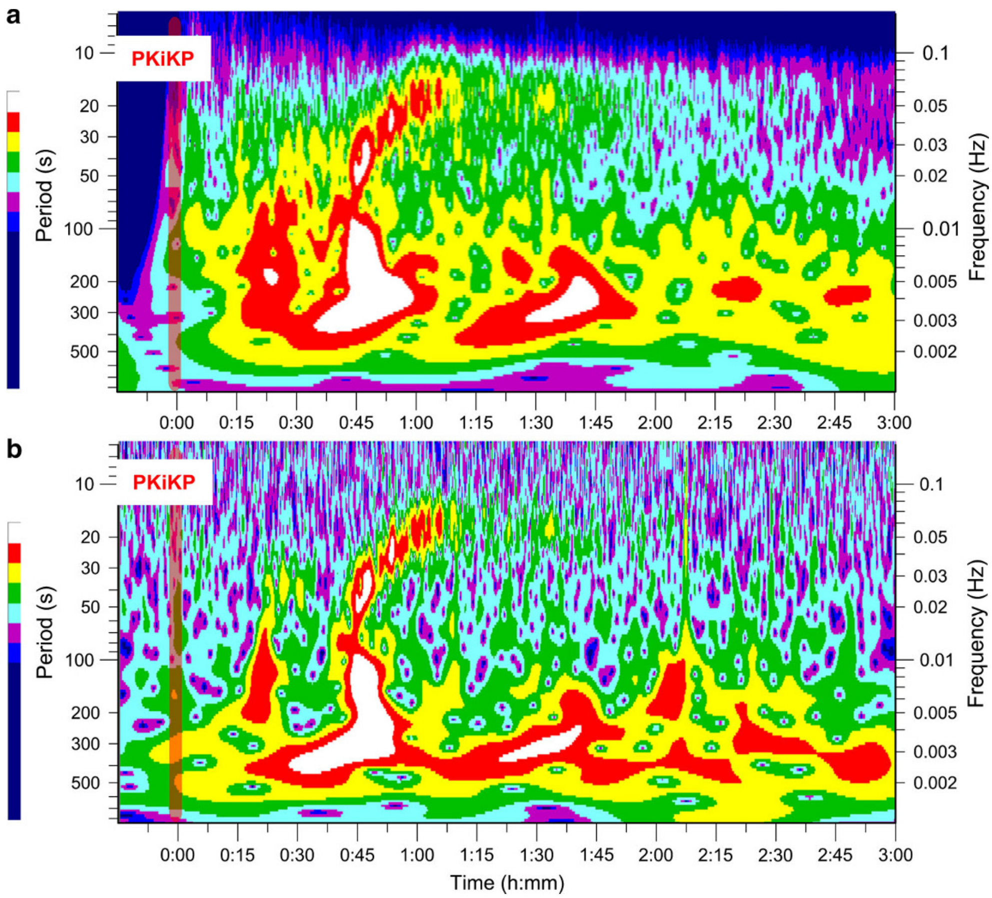

Figure 5
Morlet wavelet diagram for earthquake that occurred on February 27, 2010: **a** *GVZ* vertical ground velocity, **b** *WLC* water level response of confined aquifer. *Red line* marks PKiKP arrival and we consider this moment as a null point

background spectral ratio, both in seismic and water level records, shows that the energy of the seismic waves was concentrated at the frequency range of 0.02–0.08 Hz (Fig. 8). Much stronger seismic waves affect the unconfined aquifer in comparison to the confined one. Frequency (below 0.08 Hz) and amplitude level of oscillations of unconfined aquifer are in good correspondence with the ground velocity. The well-aquifer system poses a high-cut filter with a rather sharp slope at the frequency of 0.08 Hz. As for the low-frequency range, we see a smooth increase in the range below 0.02 Hz. Similar fluctuations (for frequencies below 0.2 Hz) were recorded by a system of wells in granitic rocks in Japan during the Chilean earthquake of February 27, 2010 (No. 1, Table 2) (Kitagawa *et al.* 2011).

WLC response induced by the passage of seismic waves of the 2015-year earthquake was concentrated at low frequencies (below 0.02 Hz). An out-of-order orange sign at 0.048 Hz in Fig. 8d corresponds to the impalpable amplification in the group of surface seismic waves, whereas a second orange sign at 0.026 Hz falls after all the values for the 2010-year earthquake with significantly greater PGV in comparison with the 2015 year event (Fig. 9). We suggest that the well-aquifer system has a frequency dependent amplification threshold to have a response to wave passage. Seismic wave needs more energy to "sway" system at higher frequencies. Exactly, this threshold case was observed for the 2015-year earthquake at a frequency 0.048 Hz (20 s) (Figs. 4d, 6c). Nevertheless, weak wave dispersion was observed on

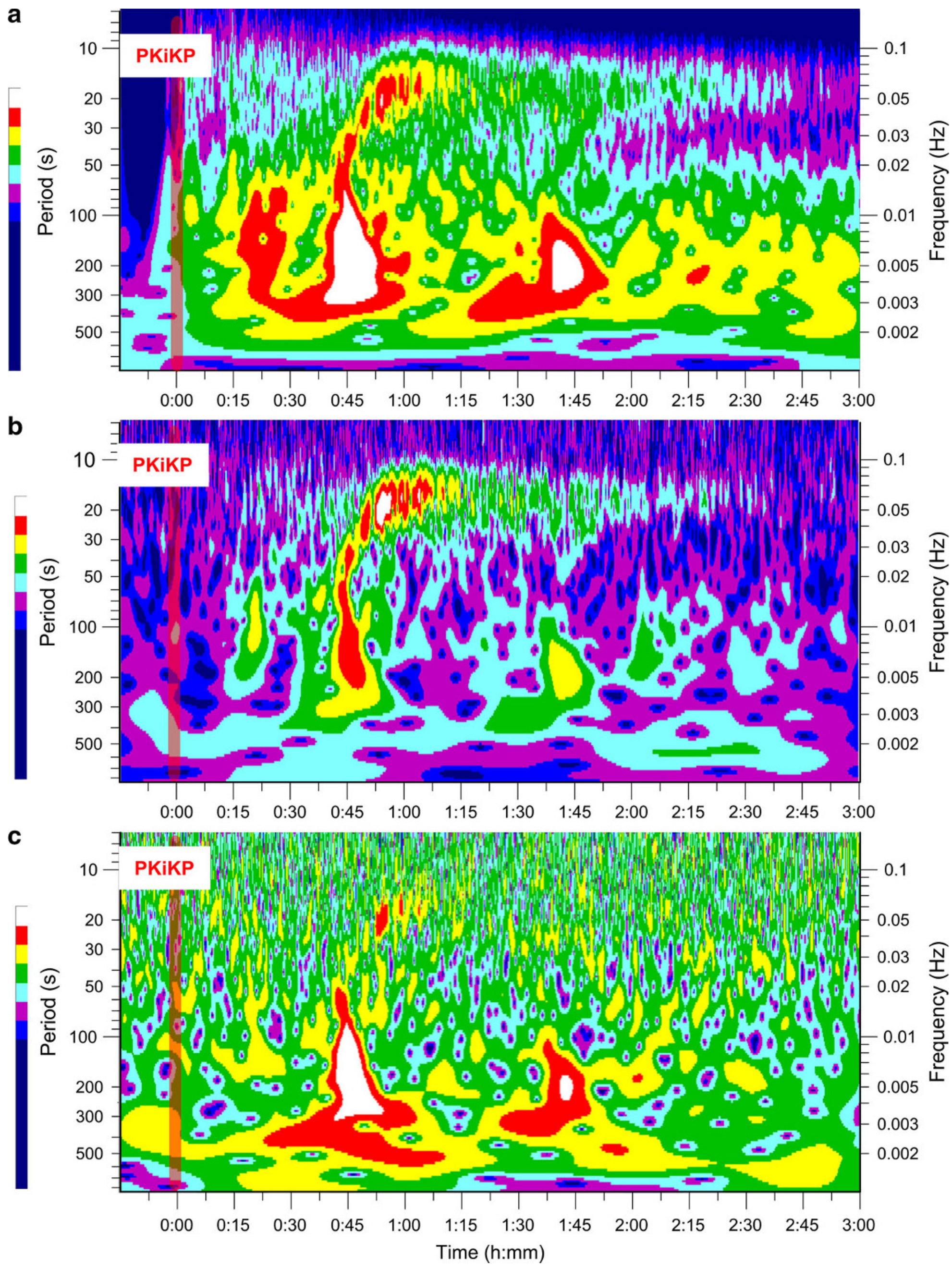

Figure 6
Morlet wavelet diagram for earthquake that occurred on September 16, 2015: **a** *GVZ* vertical ground velocity, **b** *WLU* water level response of unconfined aquifer, **c** *WLC* water level response of confined aquifer. *Red line* marks PKiKP arrival and we consider this moment as a null point

WLC response to the 2015-year earthquake as far as it existed on corresponding WLU response and WLC response to a much stronger 2010-year earthquake (time interval of 0:50–1:05 on Figs. 5, 6).

In the case under study, we found frequency-independent response either for confined or unconfined aquifer response in the period range of 15–40 s. The WLC amplification factor is about 6 mm/mm/s, and

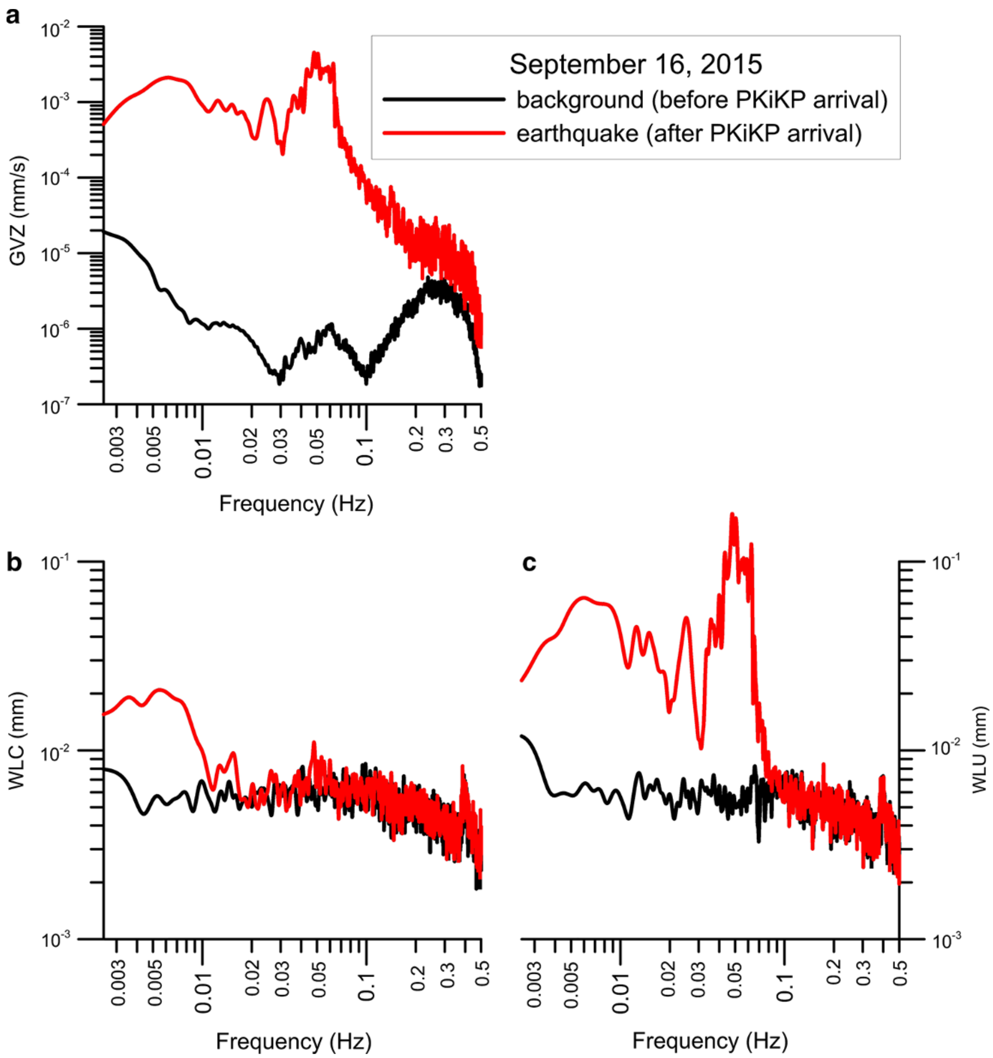

Figure 7
Spectra of microseismic noise and the water level in the wells prior to the earthquake on September 16, 2015, Ms = 8.3 before PKiKP wave arrival (*black line*) and spectra of the earthquake after PKiKP wave arrival (*red line*). *GVZ* vertical ground velocity, *WLC* water level of confined aquifer, *WLU* water level of unconfined aquifer

for WLU it is 39 mm/mm/s. WLC amplification factor is significantly less than the one for other wells, as described in literature. Thus, Brodsky *et al.* (2003) show a constant value of the amplification factor of about 200 m/m/s for periods of 20–60 s from distant earthquakes with epicentral distances of 5000–12500 km, that is 30 times more than the same at Michnevo Geophysical Observatory. As described in this paper (Brodsky *et al.* 2003), the well was drilled into a fractured granodiorite confined aquifer with hydraulic conductivity of 0.006 m/day, water column height of 83 m, and well bore radius of 0.06 m. Under our conditions water-bearing rocks consist of fractured limestones with a higher hydraulic conductivity of 0.17 m/day, but aquifer with significantly lesser pressure head (23 m) is penetrated by well with a comparable well bore radius. This confirms the dependence of the confined system amplification factor on filtration properties of an aquifer that agrees with Cooper *et al.* (1965).

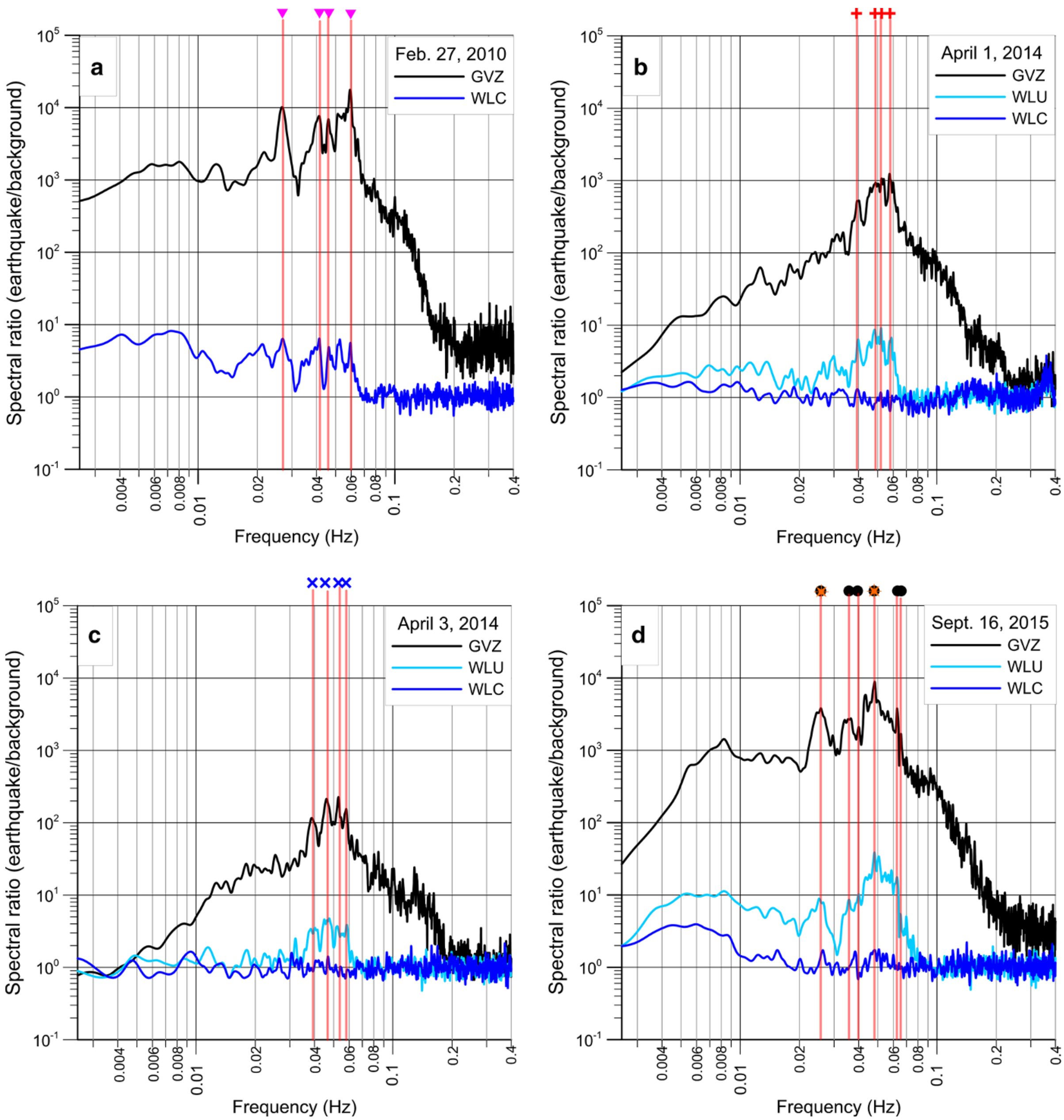

Figure 8
Spectral ratio of earthquake record (3 h after PKiKP arrival) to the natural microseismic background (3 h before PKiKP arrival): **a** February 27, 2010, Ms = 8.7; **b** April 1, 2014, Ms = 8.0; **c** April 3, 2014, Ms = 7.6; **d** September 16, 2015, Ms = 8.3. *GVZ* vertical ground velocity (*black*), *WLC* water level of confined aquifer (*deep blue*), *WLU* water level of unconfined aquifer (*light blue*). *Red lines* with signs point to significant peaks: **a** at GVZ and WLC spectra (magenta signs), **b** at GVZ and WLU spectra (*red signs*), **c** at GVZ and WLU spectra (*blue signs*), **d** at GVZ and WLU spectra (*black signs*) and at GVZ and WLC spectra (*orange signs*)

A similar theory cannot be applied for an unconfined system, but qualitatively we note that WLU transmissivity (Table 1) considerably exceeds the same for WLC as well as for the corresponding amplification factor. Moreover, two aquifers at the MHV area are characterized by different prevalence

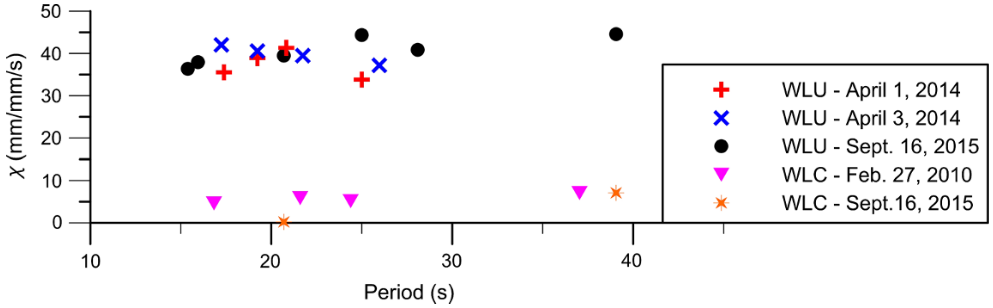

Figure 9
The amplification factor of the WLU and WLC aquifers. *Color signs* correspond to the marks in Fig. 8. For WLU aquifer: *red signs* correspond to the earthquake on April 1, 2014, *blue signs* to the earthquake on April 3, 2014, *black signs* to the earthquake on September 16, 2015. For WLC aquifer: *magenta signs* correspond to the earthquake on February 27, 2010, *orange signs* to the earthquake on September 16, 2015

area, underground water flow gradient, well depth and intersected interval. All of these physical characteristics should strongly affect aquifer response to seismic wave passage.

5. *Conclusions*

Geodynamically, the conditions of the Russian Platform allow a clear identification of the aquifer response to seismic effects of distant earthquakes. A response to the passage of the transverse and surface waves from the earthquake with Ms = 8.7 was observed in the confined aquifer. For an event with Ms = 8.3, level fluctuation was recorded only after the arrival of surface waves. In the overlying unconfined aquifer, a response to the arrival of transverse as well as of surface waves from the same event with Ms = 8.3 was observed. We suppose that the well-aquifer system response to seismic wave passage could have a frequency-dependent threshold.

It was shown that the occurrence of water level fluctuations in the well under unconfined aquifer conditions caused by distant earthquakes was determined by the PGV value and, accordingly, by the magnitude of the event. For earthquakes with magnitudes 7.1–7.2, hydrogeological response at 13000–14000 km epicentral distances was not recorded.

This study showed that medium response to dynamic impact depends on various physical parameters of the aquifers.

Acknowledgments

This work was supported by the Russian Science Foundation (Project No. 14-17-00719). The authors would like to express their sincere gratitude to Prof. G.G. Kocharyan for his indispensable advice, discussions and comments, and to N.V. Kabychenko for valuable suggestions during the work. Moreover, we thank the anonymous reviewers and editor-in-chief for their comments that helped to substantially improve the manuscript.

References

Bagmet, A.L., Bagmet, M.I., Barabanov, V.I. et al. (1989), *The study of the Earth tidal oscillations of the groundwater level in the wWell "Obninsk"*, Izv., Phys. Solid Earth *11*, 84-95 (**in Russian**).

Besedina, A.N., *Scientific substantiation methods of waveform correction vuring seismic observations: Ph.D.* (IDG RAS, Moscow 2014) (**in Russian**).

Besedina, A.N., Vinogradov, E.A., Gorbunova, E.M., and Kabychenko, N.V. (2014), *Permeability evaluation according to complex precision observations*, Seismol. Res. Lett. *85*, 2, 505.

Besedina, A.N., Vinogradov, E.A., Gorbunova, E.M., Kabychenko, N.V., Svintsov, I.S., Pigulevskiy, P.I., Svistun, V.K., and Shcherbina, S.V. (2015), *The response of fluid-saturated reservoirs to lunisolar tides: Part 1. Background parameters of tidal momponents in ground displacements and groundwater level*, Izv., Phys. Solid Earth *51*, 1, 70-79.

Bredehoeft, J.D. (1967), *Response of well aquifer systems to Earth tides*, J. Geophys. Res. *72*, 3075– 3087.

Brodsky, E.E., Roeloffs, E., Woodcock, D., Gall, I., and Manga, M. (2003), *A mechanism for sustained groundwater pressure changes induced by distant earthquakes*, J. Geophys. Res. *108*, 2390.

Brown, K.M., Tryon, M.D., Deshon, H.R., Dorman, L.M., and Schwartz, S.Y. (2005), *Correlated transient fluid pulsing and seismic tremor in the Costa Rica subduction zone*, Earth Planet. Sci. Lett. *238*, 189 – 203.

Cooper, H.H., Bredehoeft, J.D., Papdopulos, I.S., and Bennett, R.R. (1965), *The response of well-aquifer systems to seismic waves*, J. Geophys. Res. *70*, 3915–3926.

Doan M.L., Brodsky E.E., Prioul R., and Signer C. *Tidal analysis of borehole pressure - A tutorial.* (Schlumberger Research Report 2006).

Doan, M.L., and Cornet, F.H. (2007), *Small pressure drop triggered near fault by small teleseismic waves*, Earth Planet. Sci. Lett. *258* (1 – 2), 207 – 218.

Elkhoury J.E., Brodsky, E.E., and Agnew, D.C. (2006), *Seismic wave increase permeability*, Nature *441*, 1135-1138.

Kano, Y., and Yanagidani, T. (2006), *Broadband hydroseismograms observed by closed borehole wells in the Kamioka mine, Central Japan: Response of pore pressure to seismic waves from 0.05 to 2 Hz*, J. Geophys. Res., *111*, B03410, doi:10.1029/2005JB003656.

Kitagawa, Y., Koizumi, N., Takahashi, M., Matsumoto, N., and Sato, T. (2006), *Changes in groundwater levels or pressures associated with the 2004 earthquake off the west coast of Northern Sumatra (M9.0)*, Earth, Planets Space *58*, 173–179.

Kitagawa, Y., Itaba, S., Matsumoto, N., and Koizumi, N. (2011), *Frequency characteristics of the response of water pressure in a closed well to volumetric strain in the high-frequency domain*, J. Geophys. Res. Lett. *116,* B08301, doi:10.1029/2010JB007794.

Kocharyan, G.G., Vinogradov, E.A., Gorbunova, E.M., Markov, V.K., Markov, D.V., and Pernik, L.M. (2011), *Hydrologic response of underground reservoirs to seismic vibrations*, Izv., Phys. Solid Earth *47*, 12, 1071 – 1082.

Kopylova G.N., Gorbunova E.M., Boldina S.V. and Pavlov D.V. (2009), *Estimation of deformational properties of a stratum-borehole system based on analysis of barometric and tidal responses of the water level in a borehole,* Izv., Phys. Solid Earth *45*, 10, 903-911.

Liu, C., Huang, M.-W., and Tsai, Y.-B. (2006), *Water level fluctuations induced by ground motions of local and teleseismic earthquakes at two wells in Hualien, Eastern Taiwan*, Terr. Atmos. Ocean. Sci. *17*, 2, 371 – 438.

Lyubushin, A.A., Malugin, V.A., and Kazantseva, O.S. (1997), *Monitoring of tidal variations of the underground water levels in a group of water-bearing horizons*, Izv., Phys. Solid Earth *4*, 33, 302-313.

Montgomery, D.G., and Manga, M. (2003), *Streamflow and water well responses to earthquakes*, Science *300*, 27, 2047 – 2049.

SCHERBAUM F., *Of zeros and poles. Fundamentals of digital seismology* (Kluwer Academic Publishers 1996).

Shi, Z., Wang, G., Manga, M., and Wang, C.-Y. (2015), *Mechanism of co-seismic water level change following four great earthquakes – insights from co-seismic responses throughout the Chinese Mainland*, Earth Planet. Sci. Lett. *430*, 66 – 74.

Wang, C.-Y. (2007), *Liquefaction beyond the near field*, Seismol. Res. Lett. *78*, 512–517.

Wang, C.-Y., and Manga, M., *Earthquakes and water, lecture notes in Earth sciences* (Springer, Berlin 2010).

Welch, P.D. (1967), *The use of fast fourier transform for the estimation of power spectra: A method based on time averaging over short, modified periodograms*, IEEE Trans. Audio Electroacoust. *15*(2), 70–73.

(Received November 30, 2015, accepted February 13, 2016, Published online February 26, 2016)